

Effects of the NICMOS array flat-field response on observations.

C. J. Skinner
December 1, 1995

ABSTRACT

In an earlier ISR we have described the flat-field behaviour of the NICMOS array detectors, which was found to vary significantly with wavelength. In this report we use the results obtained from our detailed flat-field response tests to analyze numerically the likely effect of this behaviour on NICMOS photometry and imaging.

1. Introduction

We have shown in a previous ISR (ISR NICMOS-005) that the NICMOS array detectors exhibit rather large amplitude, wavelength dependent variations in flat-field response. The large size of these variations (a factor of four across the array at $1.2\mu\text{m}$), and their substantial variation with wavelength (from a factor of almost five at $0.8\mu\text{m}$ to a factor of only about 1.2 at $2.5\mu\text{m}$) led us to speculate that they might give rise to significant errors in photometry for sources with extreme colours. In this ISR we investigate numerically the effects of these flat-field variations on the likely photometric performance of NICMOS.

2. Modelling Technique

It should be stressed at the outset that the analysis presented here does *not* reflect the ultimate photometric performance of NICMOS or the ultimate limitations on its photometric performance. This analysis is intended to demonstrate *only* the extent to which the photometric performance of NICMOS is limited by the wavelength dependent flat-field response variations. Future ISRs will address the broader issues alluded to above.

In order to carry out this analysis, we have developed Fortran code to simulate the NICMOS images of point sources. The tasks carried out by this code are

1. approximate the spectral energy distribution in the NICMOS waveband of an arbitrary astronomical source ($F(\lambda)$);

2. multiply by the Detective Quantum Efficiency as a function of wavelength ($DQE(\lambda)$) of the detector;
3. multiply by the transmission as a function of wavelength ($T(\lambda)$) of the appropriate NICMOS filter;
4. distribute the resulting spectrum into a Point Spread Function ($PSF(x,y,\lambda)$) for the relevant NICMOS camera, distributed appropriately over the filter passband;
5. generate a number of these point source images distributed over the detector area;
6. multiply the resulting image by an appropriate flat-field image ($FF(x,y,\lambda)$);
7. simulate correcting the resulting image by an inverse flat-field response for the entire filter pass-band ($FI(x,y)$);
8. carry out aperture photometry on the images resulting from steps 5 and 7, and compare the two.

Below we briefly describe how each of these steps is accomplished.

Source Spectral Energy Distribution

This is taken to be a black-body function, with input temperature.

DQE(λ)

The measurements of the DQE for each of the 3 cameras supplied by the IDT have been used. These are tabulated at roughly $0.1\mu\text{m}$ intervals from $0.7\mu\text{m}$ to $2.3\mu\text{m}$, and at $0.02\mu\text{m}$ intervals from $2.32\mu\text{m}$ to $2.60\mu\text{m}$. Outside this waveband the detector has very low DQE. This DQE curve is simply multiplied by the black-body function.

Filter Transmission

Measurements of the filter transmissions made by the IDT at Ball during the summer of 1995 have been used. These were tabulated at 1.0nm intervals across the $0.499\mu\text{m}$ to $2.7\mu\text{m}$ waveband for most of the filters. The result of step 2 was resampled using spline interpolation onto the same wavelength grid as the filter curve, and then multiplied by it to yield the spectrum as detected by the NICMOS array. Because the source spectrum and DQE are both fairly smoothly varying functions, the spline interpolation is very well behaved, and we have verified that the interpolated function is indistinguishable from the original.

The aim of this analysis is to investigate how the variations with wavelength of the flat-field response affect photometry of sources whose spectral energy distributions rise or fall with increasing wavelength (i.e. red or blue sources). To accomplish this it is not necessary to sample the detected images at such a fine spectral resolution. Typically we only need of order ten wavelengths across the filter passband in order to accurately define the effects we

are searching for. Therefore we define an appropriate wavelength grid for each filter, and at this stage the detected spectrum is binned into this wavelength grid, and normalised to a uniform number of counts. Hence at this stage the source should have generated the same total number of counts on the detector regardless of its colour.

It should be noted that in the course of this investigation it was found that for some filters it is possible that some long wavelength photons can ‘leak’ through the filters for the very red sources (a future report will address this issue). To see how the detector responds to sources of identical detected counts, we should normalise by integrating the counts across the entire NICMOS waveband. But in doing this, the photometric accuracy we deduce will be affected by such red leaks, and an investigation of this is not the aim of this report. Therefore we have performed the normalisation, as described above, integrating only over the intended passband of the filter.

The resulting function at this stage is the detected source spectrum.

Point Spread Function

There is currently no software at STScI for generating a realistic PSF for NICMOS. We have therefore used the **tinytim** program to generate a PSF for WFPC2 through its 1.042 μm filter. We have then rescaled the resulting PSF to the size appropriate to the wavelength λ in question assuming the PSF diameter is directly proportional to λ . The pixel size of the image is also altered to be appropriate to NICMOS Camera 1 or 2. The PSF thus constructed was normalised so that its total flux was unity. A total of nine of these PSFs were written into each image, in a 3x3 grid equispaced on the array. Thus the sources appear on the array in positions determined mathematically, and do not necessarily sample the ‘best’ or ‘worst’ positions

Flat-field Response

The flat-field images used were those measured at Steward Observatory and described in NICMOS ISR-005. These images were taken through 0.1 μm bandwidth filters at wavelengths spaced every 0.1 μm from 0.8 μm to 2.5 μm . For many of the filters analysed in this ISR, sampling every 0.1 μm was quite sufficient. For a few, finer wavelength sampling was required, and in these cases we simply used linear interpolation between the measured flat-field response images.

Detected Images

To construct the images as seen by the detector, we looped over wavelength in the grid predefined for the individual filter. For each wavelength we multiplied the image consisting of nine PSFs, as described above, by the flux at the appropriate wavelength taken from the detected source spectrum, and then multiplied by the flat-field response image for the appropriate wavelength. The sum of the resultant images is the collection of nine sources

as the NICMOS detector would see them.

Corrected Image

We need to correct the image created above for the flat-field response of the filter which we are trying to simulate. Such flat-field response images have not yet been created. We have already noted that the flat-field response of the detectors is colour-dependent. Therefore it is necessary, in order to create a flat-field correction image, to specify for what colour source the image is intended to be a correction. For the purposes of this analysis we have created an inverse flat-field image appropriate for a source with neutral colour - *i.e.* a source whose flux is independent of wavelength. This was created simply by combining observed flat-field response images across the same wavelength grid as used for the detected image, weighted only by the filter response curve, and normalised to unity. The detected image was multiplied by this, resulting in an image which should simulate data that has been obtained using NICMOS and calibrated using the CALNIC pipeline code.

Photometry

The ‘perfect’ NICMOS image is represented by the collection of nine PSFs put together as described here, and summed over the wavelength grid for the filter. To simulate photometry, we sum the counts in a square aperture centred on each PSF with sides of 60 pixels. This photometry was carried out for the ‘perfect’ image and for the corrected image as described above, and the results compared to estimate how large the errors in photometry were likely to be for the chosen source colour.

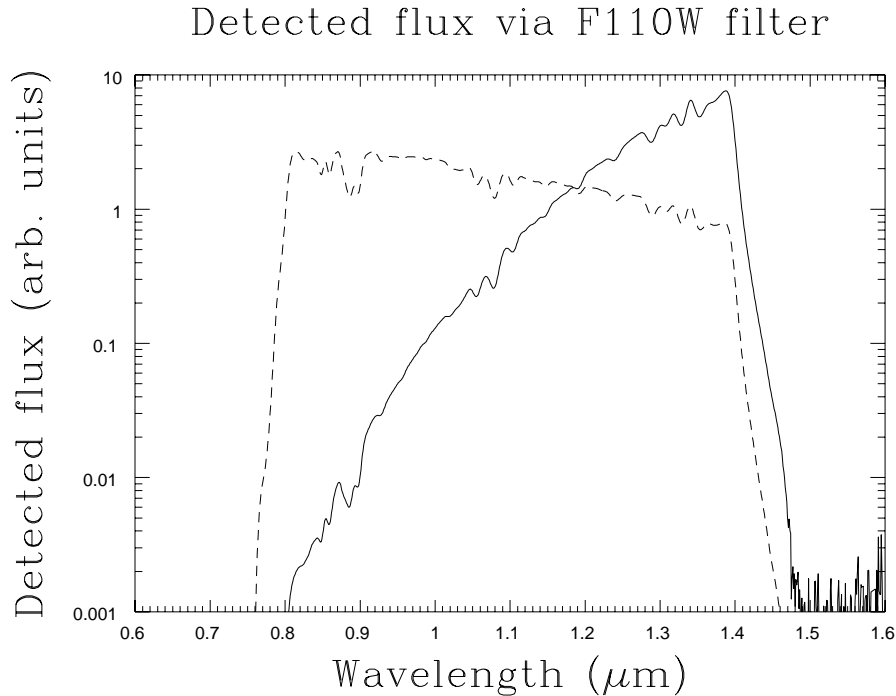
3. Results

For each filter considered, we have carried out simulated photometry as described above for sources of two different colours. The first had a colour temperature of 10,000K, and thus is typical of stellar photospheres which will comprise a significant fraction of the sources which will be detected in NICMOS images. This colour is taken to be representative of the bluer sources. The second source had a colour temperature of 700K, which is taken to be representative of the redder sources, such as embedded Young Stellar Objects (YSOs).

An example of a pair of detected spectra is illustrated in Figure 1, for the F110W filter. It can easily be seen that for this filter an image of a very red source will be dominated by the flat-field response image in the 1.2-1.4 μ m waveband, while for a blue source the most important contribution will come from the 0.8-1.0 μ m (although for stellar photospheres the spectral index is simply not large enough for the image to be dominated by the flat-field response in any small waveband; instead contributions are made by the flat-field response across the whole filter bandpass).

For the same filter, we show in Figure 2 the flat-field response images obtained at Steward,

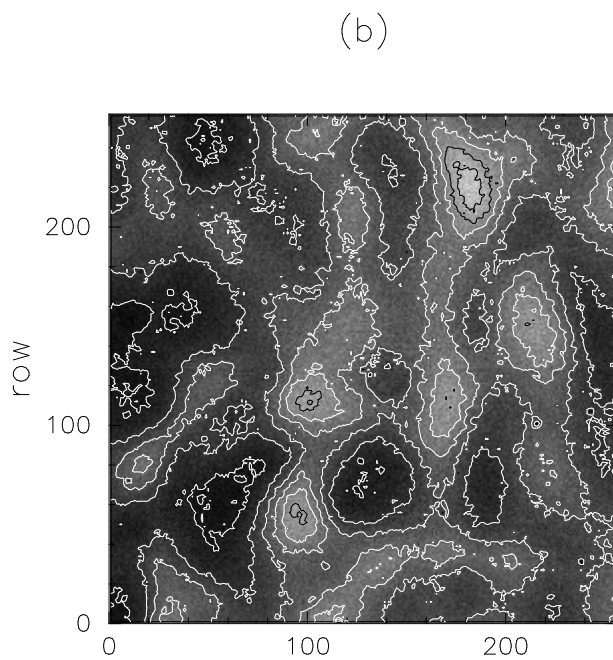
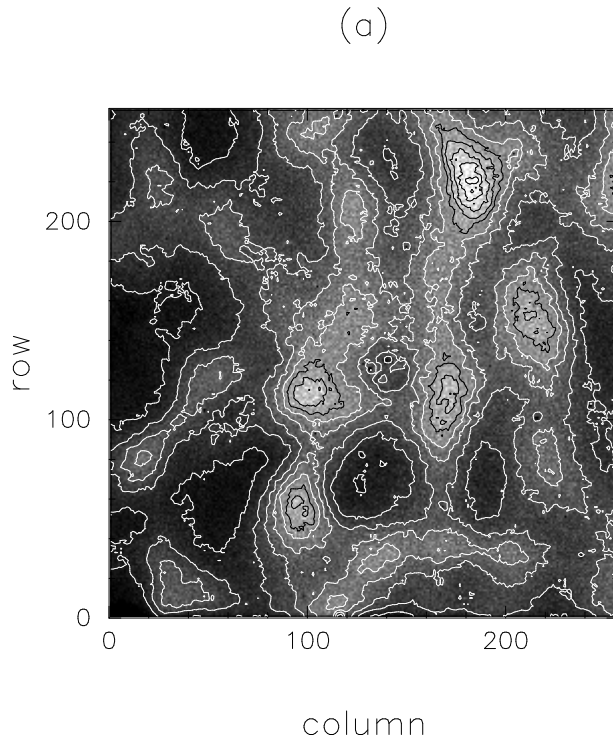
Figure 1: the detected source spectrum, for sources with colour temperatures of 700K (solid line) and 10,000K (dashed line). It is easy to see that the detected image will be dominated by the flat-field response in the 1.2-1.4 μ m region for a 700K source, while for a 10,000K source the detected image will be affected by the flat-field response throughout the filter bandpass.



using 0.1 μ m bandwidth filters, at 0.8 μ m and 1.4 μ m. It can be clearly seen that there is a significant change in flat-field response variations between the two wavelengths, so that photometry of sources with radically different colours using this filter may be expected to accrue some errors. For a source with neutral colours, the appropriate flat-field response to use for correcting an image would be intermediate between the two images discussed above.

The results of our photometry are summarised in Table 1. For each filter considered, we list the error in photometry accrued by sources with colour temperatures of 10,000K and 700K, when the images are corrected using an inverse flat-field image appropriate for a source with neutral colour. Tests indicated that we are able to determine the photometric accuracy of an image using the techniques described here to considerably better than 0.1%. However, we consider that photometric errors of less than 0.1% are of no consequence so far as this report is concerned. We list the results only for the broad-band filters and for those medium bandwidth filters whose passbands lie in or close to the regions where the flat-field response variations are changing rapidly with wavelength, at either end of the NICMOS waveband. We have performed this analysis on a number of the other medium bandwidth filters, and find that the errors introduced by flat-field effects are negli-

Figure 2: flat-field response images for $0.8\mu\text{m}$ (a) and $1.4\mu\text{m}$ (b), wavelengths at the extrema of the F110W bandpass. Contour and grey-scale settings are identical for the two images, and both linear. Clearly there is a significant change in the flat-field response between these two wavelengths, so that sources with extreme colours may be expected to generate erroneous photometry for this filter.



gible, as expected, for these filters. The filters listed are the only ones for which any significant errors arise.

Table 1:

Filter	Error for 10,000K	Error for 700K
F090M	<0.1%	1.9%
F110W	1.1%	2.9%
F140W	0.7%	3.1%
F160W	<0.1%	0.3%
F187W	<0.1%	0.3%
F205W	0.4%	2.1%
F222M	<0.1%	0.1%
F240M	1.0%	0.9%

4. Discussion

The photometric accuracy achievable with straightforward correction of an image using a static database inverse flat-field is much better than would have been expected based on J and K band flat-field images. It is clear from the data presented in ISR NICMOS-005 that the great majority of the variation in flat-field response evident in the J and K band data actually arises inside the K bandpass. Therefore predictions of the photometric accuracy possible based on a linear extrapolation/interpolation from the J and K band data were much more pessimistic than the results obtained here. The spectral behaviour of the flat-field response of the detectors, *i.e.* large variations only at the extreme ends of the NICMOS bandpass where there are no broadband filters, and very stable behaviour between, is indeed fortunate.

It might have been expected that the filters at the extreme wavelengths, namely the F090M, F222M and F240M filters, would have much bigger photometric errors than are being presented here. In practise, however, the bandwidth of these filters is small enough that the variation in brightness of an object within the bandpass, even one with rather extreme colours, is not large enough to cause significant problems. Not surprisingly, the largest errors arise in the 3 broadband filters whose bandpasses include some part of the regions where the flat-field response changes most rapidly.

The photometric errors derived here are not particularly large. However, for observers requiring high precision photometry, these represent non-trivial limits beyond which it will not be possible to venture without obtaining multi-wavelength images. Added to a variety of other possible sources of error, these flat-field effects will provide significant

limits.

It will certainly be possible to improve upon the accuracy suggested here. In order to obtain 1% precision using the F110W filter, for instance, observers should observe at a minimum of one other wavelength. The colour information derived from the pair (or multiplet) of images could then be used to construct a more appropriate flat-field image, which could then be applied to improve the colour information, and so on. Such an iterative technique will probably be used in an IRAF task to be provided for the accurate flat-field correction of NICMOS images.

The two colour temperatures used here were 10,000K and 700K. The choice of temperatures is very subjective, and open to question. The hotter of the two corresponds, in the NICMOS waveband, to the Jeans tail of a stellar photosphere, which is the bluest spectral energy distribution likely to be commonly encountered in NICMOS images. However, it is worth noting that for reflection nebulae illuminated by hot stars, a significantly steeper (bluer, in other words) spectrum is often seen. However, such sources are not particularly common, and to obtain a reasonable estimate of the *typical* errors we have used the stellar photospheric case. A 700K colour temperature corresponds in ground-based photometric terms to $J-K=5$. This is a colour encountered fairly commonly in embedded YSOs. There are again well-known examples of even redder sources - the Becklin-Neugebauer object, for example, has no published photometry at J, but has $H-K=4.1$, and the massive YSO AFGL2591 has $J-K=6.0$. YSOs with $J-K=7$ are known, although not in large numbers. Using $J-K=5$ seems to us to give a fair indication of the likely photometric uncertainties, and in practise such objects are already so red that using more extreme sources increases the uncertainties by a rather small amount.

The analysis and discussion has been limited to point sources, but some mention should be made of the situation for extended objects. A good example to discuss would be the aforementioned YSO AFGL2591. This has an extremely red core, whose $J-K=6$ and which is entirely undetected optically. However, it also has a large IR nebula which is quite prominent at J and K, and in the red visual region, but much fainter at L, and which is probably largely reflection nebulosity. The nebula has highly variable colour, some parts of it having fairly neutral or even slightly blue colours in the NICMOS waveband, while other parts are extremely red. Obtaining very accurate measurements of the colour of such a source would require the use of images at more than one wavelength and an iterative tool of the kind described earlier. A further example of this kind of complicated object is the prototypical post-AGB object CRL2688, the Cygnus Egg Nebula, which has an extremely blue bipolar reflection nebula surrounding an extremely red core. Techniques which require very accurate measurements of the surface brightness of extended objects, such as the brightness fluctuation technique for distant galaxies, will need to be applied with care given to the photometric uncertainties such as those discussed here.

5. Conclusions

- For the broadest NICMOS filters, and for those at extreme wavelengths, the wavelength dependence of the flat-field response generates photometric errors for sources of unknown colour.
- The sizes of these errors are small, typically less than 3%.
- These errors can be corrected if more accurate photometry is needed, by taking multi-wavelength observations and using an iterative correction technique.